

# Optimization of process variables on Electrical Discharge Machining of novel Al7010/B<sub>4</sub>C/BN hybrid metal matrix nanocomposite

Gopichand Dirisenapu<sup>1\*</sup>, Laxmanaraju salavaravu<sup>2</sup>, Murahari kolli<sup>3</sup>, Rajyalakshmi Bandi<sup>4</sup>, Ashish kumar sahu<sup>5</sup>, Kosaraju Satyanarayana<sup>5</sup>

<sup>1</sup>Panchayat Raj Engineering Department, Andhra Pradesh, India

<sup>2</sup>Department of Mechanical Engineering, Sri Sivani College of Engineering, Etcherla, India

<sup>3</sup>Department of Mechanical Engineering, Lakireddy Balireddy College of Engineering (A), Mylavaram, India

<sup>4</sup>Department of Electronics and Communication Engineering, DVR & Dr. HS MIC College of Technology (A), Kanchikacharla, India

<sup>5</sup>Department of Mechanical Engineering, IIT Delhi india

<sup>6</sup>Gokaraju Rangaraju Institute of Engineering and Technology, Hyderabad, India

**Abstract.** In this paper, determination of optimum EDM input variables like discharge current (DC), pulse on time (Pon), pulse off time (Poff), and gap voltage (GV) on responses like material removal rate (MRR) and surface roughness (SR) using Taguchi technique on the novel Al7010/2%B<sub>4</sub>C/2%BN hybrid metal matrix nanocomposite (HMMNC) manufactured through ultrasonic assisted stir casting (UASC) route. The various experiments were planned and carried out L<sub>16</sub> orthogonal array and regression equations were established by using Analysis of variance (ANOVA) to examine the impact of pulse factors. The outcomes exposed that discharge current greatest effect factor on MRR and SR was found with % contribution of 82.07% and 86.86%. It is also identified that the optimum level conditions of pulse factors for MRR and SR is A<sub>4</sub>B<sub>4</sub>C<sub>1</sub>D<sub>1</sub> and A<sub>1</sub>B<sub>1</sub>C<sub>4</sub>D<sub>4</sub>. The outcomes were further determined by utilizing confirmatory experiment. The machined surface morphology was observed through Scanning electron microscope (SEM).

## 1. Introduction

Aluminum metal matrix nanocomposites (AMMNCs) are becoming increasingly popular in industries such as automotive, aerospace, and nuclear due to their desirable characteristics, like high stiffness, superior strength, low density, corrosion resistance, and excellent electrical and thermal conductivity.

---

\*Corresponding author: [dchandu310@gmail.com](mailto:dchandu310@gmail.com)

These materials are considered advanced and novel due to their unique combination of characteristics [1]. The B<sub>4</sub>C and BN nanoparticles are used as reinforcements which lead to improve the properties for the nanocomposites. The even spreading of nanoparticles in the AMMNCs, during the preparation of AMMNCs is the most critical factor for getting excellent superior properties of the AMMNCs [2]. The nanoparticles are very difficult to attain an even distribution in the AMMNCs. Because of the different reasons of the different manufacturing process the nanoparticles were formed in the clusters or agglomerations. According to some literature, the UASC route is considered a preferable manufacturing technique for producing AMMNCs due to its ability to effectively wet and distribute nanoparticles within the aluminum alloy. [3-4]. The conventional machining routes are not efficient due to the mixing of ceramic hard particles in the aluminium alloy. Therefore, the unconventional machining would be a superior and good decision to machine such hard and critical to-cut materials. The EDM route is supreme conspicuously utilized unconventional machining route used to machine for all intents and purposes any material into typical or complex shapes with high dimensional exactness and accuracy, which by conventional processes would be extremely costly or even difficult to accomplish. EDM is a thermo-electric machining process that entails the expulsion of material from a workpiece (WP) as a result of the energy generated by sparks formed in the gap between the electrode and WP, which is submerged in a dielectric oil. An advantage of the EDM route is that it is capable of machining a wide range of workpiece materials, irrespective of their physical and mechanical characteristics [5]. The selection of the appropriate EDM input variables is a crucial job that enhances the machining properties. Singh et al. studied the working of EDM factors on machining of 10 SiC hybrid composite was manufactured by using stir casting method. The influence of process variables is Current, Pon and Tool material. The investigated the three output responses, namely, MRR, TWR and SR. The best machining characteristics was identified at DC (10A), Pon (120 $\mu$ m), GV (4V) and copper tool material for maximum MRR, minimum SR & TWR [6]. Palanisamy et al. optimized the input parameters like DC (A), Pon (B) and Poff (C) for getting optimum performance factors such as TWR, MRR and SR by using GRA. The LM6-Al<sub>2</sub>O<sub>3</sub> stir casted composite is used in this study. The outcome revealed that DC is the best prominent parameter that affects the SR & MRR [7].

Gopalakannan et al. observed the influence of DC, Poff, GV, and Pon and on response variables like EWR, MRR and SR in EDM of Al<sub>70</sub>75-10%B<sub>4</sub>C composite. The determinations exposed that the Pon and DC was the best significant parameters that affected the MRR. The MRR first enhanced and then decreased with a rising Pon. The increasing SR with a rise in Pon and DC and SR first reduced but further enhance in GV outcome in a rise in SR [8]. Daneshmand et al. investigated the comparison between machining of Al/Al<sub>2</sub>O<sub>3</sub> composites with various volumes of Al<sub>2</sub>O<sub>3</sub> and an Al<sub>20</sub>24 alloy was examined by using EDM. The conclusions exposed that incorporation of Al<sub>2</sub>O<sub>3</sub> particles in to the composites and DC and Pon substantial has substantial influences on the SR, TWR and MRR. The rise in current and Pon with SR, TWR and MRR was increased [9]. Nanimina et al. determined the impact of EDM on Al<sub>60</sub>61/30% Al<sub>2</sub>O<sub>3</sub> composites. The DC, Poff, and Pon were selected as process factors in this evaluation. The outcomes indicated that rise in DC intensity enhances MRR and TWR and also revealed that Pon and DC are most significant variables affecting the TWR & MRR [10]. Kumar et al. examined the impact of EDM control variables on output parameters like EWR, MRR, and SR during EDM route of Al-B<sub>4</sub>C composite. The investigations showed that current is the supreme affecting variable on SR and MRR and the main factor for EWR is material used for electrode. The ANOVA showed the similar conclusions [11]. Senthilkumar et al. determined the influence of I<sub>p</sub> (A), Pon and F<sub>p</sub> on output parameters of MRR and TWR during EDM machining of Al-TiC MMC with varying Wt.% (2.5 and 5) of TiC. In these processes, kerosene is a dielectric fluid and electrode is 7 mm copper rod. The performances revealed an increased MRR with rise in Wt.% of TiC

particles in the AMMCs. The MRR and TWR are affected by  $I_p$ .  $F_p$  plays a significant role in continuing the machining and enhancing the MRR at higher  $I_p$  and Pon duration [12]. Kathiresan et al. evaluated the influence of DC and various volume fractions SiC particles reinforced composites on response factors like SR and MRR. The pressure die casting with vortex motion method is used for preparing the Al-SiC composites. The investigations exposed that the SR and MRR was risen with reduce in current. The enhance in Wt% of SiC with MRR was enhanced [13].

The aim of the present research evaluating optimum EDM process conditions on EDM performance properties like MRR, TWR and SR by using Taguchi technique. This evaluation is conducted on Al7010/2%B4C/2%BN hybrid metal matrix nanocomposite, which is manufactured through UASC method. The four control factors were selected in this present examination are DC, Pon, Poff, and GV. In order to evaluate the % of contribution of each control factor towards the output variables, the ANOVA test was utilized. Additionally, the microstructural changes on the EDM surfaces of the WPs were examined by using a SEM.

## 2. Materials and Manufacturing process

### 2.1. Material preparation

In this paper, Al7010 alloy as the base material, nanoparticles as the reinforcement particles. the Al7010 alloy and nanoparticlessis procured from paraswaminimetals, Mumbai, india. The Al7010/2%B4C/2%BN HMMNC is fabricated using UASC processes. The mechanical properties of Al7010/2%B4C/2%BN HMMNC are summarized in Table 1.

**Table 1:** Mechanical characteristics of the AHMMNC.

S No.	Composite Composition	UTS (MPa)	YTS (MPa)	% Elongation	Microhardness (HV)
1	AA7010-2%B4C-2%BN	227.089	218.56	1.022	172.72

### 2.2. Taguchi method

The Taguchi method is a strategy for optimizing processes that is cost-effective and employs a systematic and efficient approach. The method is primarily based on two tools: orthogonal arrays, which allow for the selection of input factors with various levels, and design of experiments, which involve conducting experiments and determining response parameters using signal-to-noise ratio properties. The S/N ratio properties can be either 'the higher, the better' or 'the lower, the better'. Equations 1 and 2 are utilized to determine the N ratios for these characteristics, respectively. This approach decreases the number of experimental runs required compared to other techniques. By reducing fabrication costs and time, the method produces high-quality products [15-16]. The chosen control variables are listed in Table 2.

$$\eta = -10 \log_{10} \left[ \frac{1}{n} \sum_{i=1}^n \frac{1}{y_i^2} \right] \text{----- (1)}$$

$$\eta = -10 \log_{10} \left[ \frac{1}{n} \sum_{i=1}^n y_i^2 \right] \text{-----} (2)$$

Where,

$\eta$  = S/N ratio of experimental values,  $y_i$  = experimental values of the  $i$ th experiment and  $n$  = total number of experiments.

The software Minitab17.0® was used to determine the characteristics, and the S/N ratio values for each experiment in the L16 (4<sup>4</sup>) orthogonal array for MRR & SR of the AHMMNC are presented in Table 3. To assess the significance of each control parameter, ANOVA was identified to determine the % of contribution.

**Table 2.** pulse factors and their levels.

Input parameters	Units	Levels			
		1	2	3	4
Discharge current (A)	A	2	4	6	8
Pulse on time (B)	µs	15	30	45	60
Pulse off time (C)	µs	10	25	40	55
Gap voltage (D)	V	30	40	50	60

**Table 3** Experimental layout using an L16 OA and experimental results of MRR and SR.

S No	Discharge current (A)	Pulse on time (µs)	Pulse off time (µs)	Gap voltage (V)	MRR (g/min)	SR (µm)
1	2	15	10	30	0.064	6.59
2	2	30	25	40	0.063	6.2
3	2	45	40	50	0.068	6
4	2	60	55	60	0.052	6.24
5	4	15	25	50	0.079	6.35
6	4	30	10	60	0.091	6.34
7	4	45	55	30	0.089	7.07
8	4	60	40	40	0.103	7.35
9	6	15	40	60	0.080	7.82
10	6	30	55	50	0.090	7.96
11	6	45	10	40	0.114	8.79
12	6	60	25	30	0.116	9.74
13	8	15	55	40	0.106	9.96
14	8	30	40	30	0.133	10.65
15	8	45	25	60	0.127	10.13
16	8	60	10	50	0.157	10.95

### 2.3. Experimental procedure

The EDM experiments were conducted using the SPORKONIX EDM S 65 machine is shown in Figure 1. The EDM has servo control system to facilitate upward and down ward

movement of the electrode and jet flushing system for flushing of dielectric fluid on to the WP and electrode. The electrode material used in the process is pure electrolytic copper with a diameter of 10 mm, and it has a purity of 99.9%. EDM oil is used as the dielectric fluid. A rectangular plate with dimensions 120mm x 60mm x 6mm is used as the workpiece material. The machining depth of 1 mm is maintained throughout the experimentation work. The experimental details of EDM are indicated in Table 2 and 4. The machines specimen of the nanocomposite is shown in Figure 2.

SEM, model JEOL, JSM-660LV with EDS is used for the microstructural analysis of the composite material. The XRD analysis of the materials is obtained from X'pert PRO PAN analytical diffractometer with CuK $\alpha$  radiation apparatus.

**Table 4:** Experimental Details.

Experimental Facility	Specifications
EDM	Sparkonix (Bangalore, India)
Tool	Copper rod (10mm diameter and 110mm length)
Flushing pressure	1.25 kg/cm <sup>3</sup>
Dielectric fluid	EDM oil (Viscosity CST at 30°C
Machining time	30 min

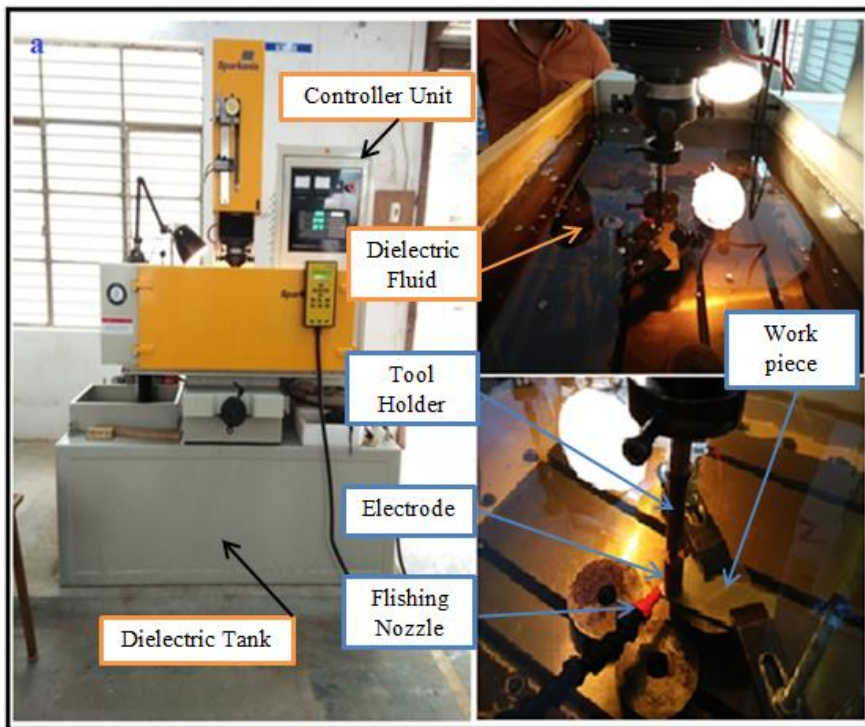


**Figure 1.** Electrical discharge machine.



**Figure 2.** Machined Specimen of the nanocomposites.

The investigations are conducted by employing a one variable at a time approach, where the control factors, such as DC (A), Pon ( $\mu$ s), Poff ( $\mu$ s), and GV (V), are modified individually, with the goal of assessing the output characteristics, including SR and MRR. To measure the SR of the machined AHMMNC, a portable surface roughness tester (Talysurf) is utilized. The MRR is determined as the ratio of the amount of WP material removed to the machining time and is calculated using the below-mentioned formula. The weight of the material that is eliminated through machining is evaluated using a high-precision weighing balance (Shimatzu (AUX120)) that has an accuracy level of 0.0001 grams.

$$\text{MRR (g/min)} = \frac{W_{wb} - W_{wa}}{T_m(\text{min})}$$

Where,  $W_{wb} - W_{wa}$  = weight difference of work piece, and  $W_{tb} - W_{ta}$  = weight difference tool.

$T_m$  is machining time.

### **3. Results and Discussions**

#### **3.1. Microstructure of the AHMMNC**

Figure 3 (a) shows the SEM image of the Al7010/2%B4C/2%BN HMMNC, which reveals the even dispersion of B4C & BN nanoparticles in the Al7010 matrix. Uniform dispersion of B4C & BN nanoparticles is essential for achieving the desired mechanical properties in the AHMMNC. Additionally, the SEM images also indicate the absence of casting faults such as porosity and oxide inclusions. Figure 3 (b) presents the EDS analysis of the Al7010/2%B4C/2%BN HMMNC. The figure shows a high peak for Al alloy and low peaks for boron, carbon, and nitrogen.

The phase purity of AA7010/B4C/BN HMMNC is determined using XRD. The XRD analysis graphs are shown in Figure 4. The results reported presence of base matrix observed by strong and long peaks, and B4C and BN particles with small peaks. The XRD pattern also shows the purity of the AHMMNC without any oxidation reaction during the production of the composite.



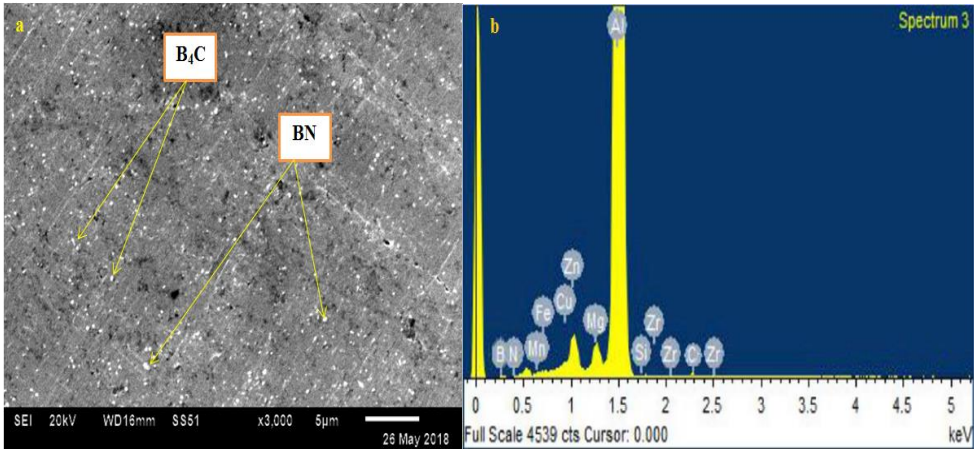


**Figure 3 (a-b)** SEM micrograph and EDS Spectrum of the AHMMNC.

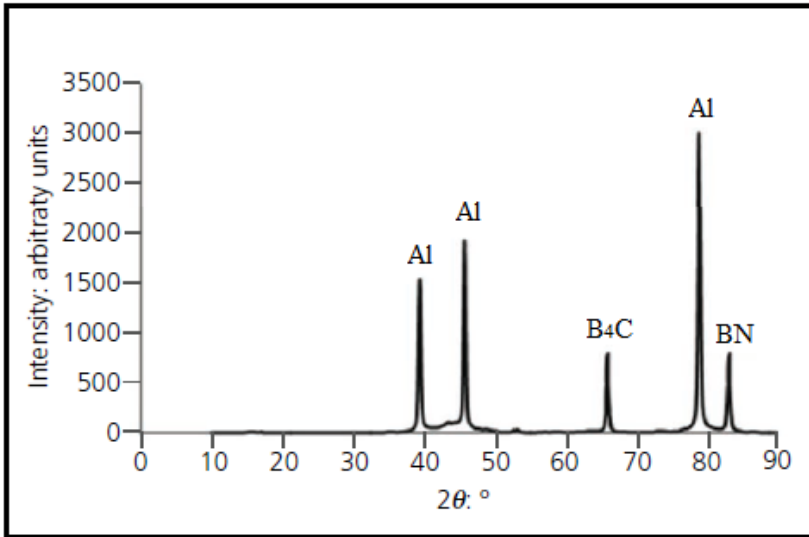


**Figure 4** XRD Patterns of AHMMNC.

### 3.2. Material removal rate (MRR)

#### 3.2.1. Effect of EDM pulse variables on MRR

Table 5 displays the S/N ratio values for MRR, while Table 6 illustrates the impact of each input pulse factor. The findings suggest that DC had the greatest delta value and was rated as the most noteworthy factor for MRR. The remaining pulse variables, namely Pon, Poff, and GV, trailed DC in terms of their impact on MRR.

**Table 5** Experimental outcomes and S/N ratios of EDM.

S No	Discharge current (A)	Pulse on time (µs)	Pulse off time (µs)	Gap voltage (V)	MRR (g/min)	S/N Ratio	SR (µm)	S/N Ratio
1	2	15	10	30	0.064	-23.90	6.59	-16.38
2	2	30	25	40	0.063	-23.97	6.2	-15.85
3	2	45	40	50	0.068	-23.41	6	-15.56
4	2	60	55	60	0.052	-25.63	6.24	-15.90
5	4	15	25	50	0.079	-22.01	6.35	-16.06
6	4	30	10	60	0.091	-20.86	6.34	-16.04
7	4	45	55	30	0.089	-20.98	7.07	-16.99
8	4	60	40	40	0.103	-19.76	7.35	-17.33
9	6	15	40	60	0.080	-21.90	7.82	-17.86
10	6	30	55	50	0.090	-20.89	7.96	-18.02
11	6	45	10	40	0.114	-18.84	8.79	-18.88
12	6	60	25	30	0.116	-18.74	9.74	-19.77
13	8	15	55	40	0.106	-19.53	9.96	-19.97
14	8	30	40	30	0.133	-17.50	10.65	-20.55
15	8	45	25	60	0.127	-17.94	10.13	-20.11
16	8	60	10	50	0.157	-16.06	10.95	-20.79

**Table 6** Response table for MRR.

Levels	Discharge current (A)	Pulse on time (B)	Pulse off time (C)	Gap voltage (D)
1	-24.23	-21.84	-19.92	-20.28
2	-20.90	-20.81	-20.67	-20.52
3	-20.09	-20.29	-20.64	-20.59
4	-17.76	-20.05	-21.76	-21.58
Difference	6.47	1.79	1.84	1.30
Rank	1	3	2	4

The main plots for S/N ratio are displayed in Figure 5. In that Figure the impact of various machining variables, like DC, Pon, Poff and GV on MRR was indicated. The DC increases with MRR were increased. The rise in current causes rise in discharge energy with the enhancement in impulsive forces on the machining region of the work piece resulting in higher melting temperature and hence higher MRR [11]. As Pon rises, more energy is supplied on to the workpiece (WP) which results in enhance in MRR. There is a proportional relationship between Pon and MRR in EDM. An enhance in Pon leads to an increase in the amount of energy supplied, resulting in higher discharge energy. This increase in discharge energy results in more metal being removed from the WP, there by enhances the MRR. This



information has been provided without plagiarism. [17]. The Poff rises with decreased in MRR. The Poff enhances the energy supplied on the WP was low due to that the MRR was reduced. The MRR reduced with an enhance in gap voltage. The GV rises the energy supplied on the WP was low because of the reduced in MRR. The increasing voltage with MRR was reduced because of lower energy supplied between the tool and WP [18]. The maximum MRR is attained when using level 4 for DC, level 4 for Pon, level 1 for Poff, and level 1 for GV. Therefore, the optimal levels of the various factors for achieving maximum MRR is A4B4C1D1.

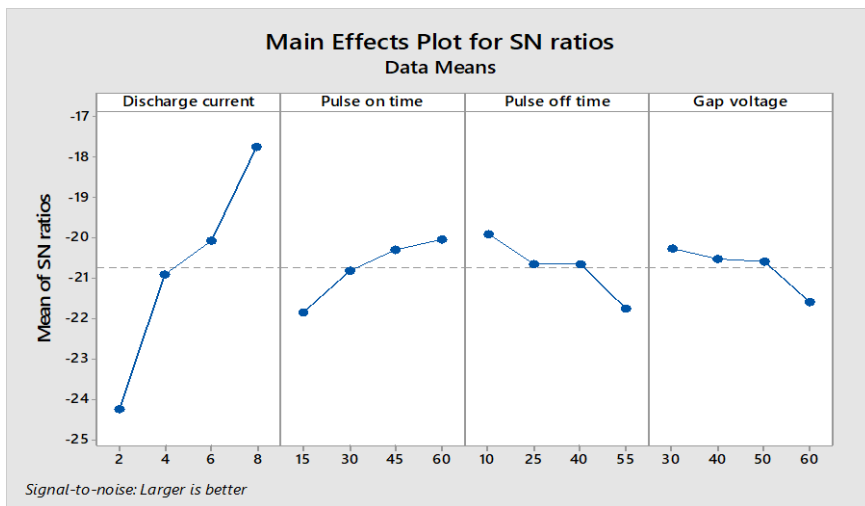


Figure 5 Main effects plots for S/N ration for MRR.

### 3.2.2. Analysis of ANOVA

ANOVA was employed to assess the importance of the pulse factors on the response parameters of MRR and to evaluate the % of contribution of the control factors on EDM responses. The outcomes of the ANOVA are presented in Table 7, which reveals that DC is the most significant variable, contributing to 82.07% of the MRR response. The other variables, including Pon (7.21%), Poff (6.60%), and GV (3.76%), followed DC in terms of their contribution to MRR. The ANOVA was conducted with a confidence level of 95%, and a "p" value less than 0.05 was considered significant. Therefore, DC, Pon, Poff, and GV significantly influenced MRR.

Table 7 ANOVA results for MRR.

Process parameter	DF	Seq SS	Adj SS	Adj MS	F Value	Pvalue	% Cont
Discharge current (A)	3	85.954	85.954	28.6515	238.51	0.0003	82.07
Pulse on time (B)	3	7.552	7.552	2.5173	20.95	0.0160	7.21
Pulse off time (C)	3	6.914	6.914	2.3048	19.19	0.0180	6.60
Gap voltage (D)	3	3.948	3.948	1.3159	10.95	0.0400	3.76
Error	3	0.360	0.360	0.1201			0.34
Total	15	104.729					100

### 3.3. Surface roughness (SR)

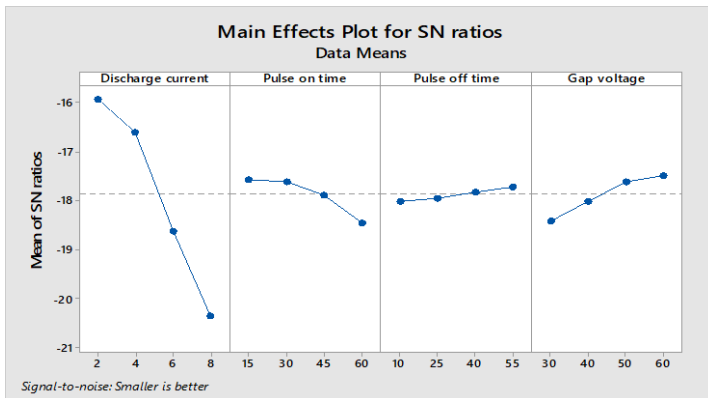
**3.3.1. Effect of EDM pulse variables on SR**

Table 5 indicates the calculated value of S/N ratio for SR, while the contribution of each control pulse factors is indicated in Table 8. The DC was getting highest delta value and first rank. The current is best substantial parameter for SR followed by other pulse variables like Pon, Poff and GV.

**Table 8** Response table for SR.

Levels	Discharge current (A)	Pulse on time (B)	Pulse off time (C)	Gap voltage (D)
1	-15.92	-17.57	-18.02	-18.42
2	-16.60	-17.61	-17.95	-18.00
3	-18.63	-17.89	-17.82	-17.61
4	-20.35	-18.45	-17.72	-17.48
Difference	4.43	0.88	0.30	0.94
Rank	1	3	4	2

Figure 6 displayed the main plots for S/N ratio. In that Figure the influence of various machining variables, like DC, Pon, Poff and GV on SR was indicated. The discharge current rises the SR enhances. The amount of thermal energy that is utilized to remove material during the EDM process is largely dependent on the DC. The increase in DC reasons a rise in the discharge heat energy and forms a pool of molten material which exists in the overheated form. These outcomes the SR was increased [12]. The Pon increase with SR was increased. The amount of material removed from the workpiece during the EDM process is directly proportional to the amount of energy that is supplied during the machining operation. These outcomes in producing a rough surface as this energy are enhanced. The Poff enhances with decreased in SR. The Poff rises the plasma channel formed in the discharge gap is high and the bombarding impulsive forces of energy is high due to high transfer of ions [19]. The GV increase with SR was reduced. The low values of voltage the SR was obtained low. The rise in GV leads to decrease in SR. The minimum SR is achieved at level 1 for DC, level 1 for Pon, level 4 for Poff, and level 4 for GV. The optimal level of various factors for minimizing SR is A1B1C4D4.



**Figure 6.** Main effects plots for S/N ratio for SR.

**Table 9** ANOVA results for SR.

Process parameter	DF	Seq SS	Adj SS	Adj MS	F Value	Pvalue	% Cont
Discharge current (A)	3	48.5790	48.5790	16.1960	1302.03	0.000	91.71
Pulse on time (B)	3	1.9660	1.9660	0.6553	52.69	0.004	3.71
Pulse off time (C)	3	0.2142	0.2142	0.0714	5.74	0.093	0.40
Gap voltage (D)	3	2.1714	2.1714	0.7238	58.20	0.004	4.10
Error	3	0.0373	0.0373	0.0124			0.07
Total	15	52.9679				Total	100

### 3.3.2. Analysis of ANOVA

Table 9 illustrates the application of ANOVA to evaluate the significance of pulse variables on SR response factors and the % contribution of input factors to EDM responses. The outcomes indicate that the DC is the most vital variable (86.86%), followed by Pon (9.15%), Poff (1.08%), and GV (0.16%). ANOVA was conducted with a confidence level of 95%, and a p-value lower than 0.05 was considered statistically significant. The DC was found to have a significant impact on SR, while Pon, Poff, and GV had an insignificant effect.

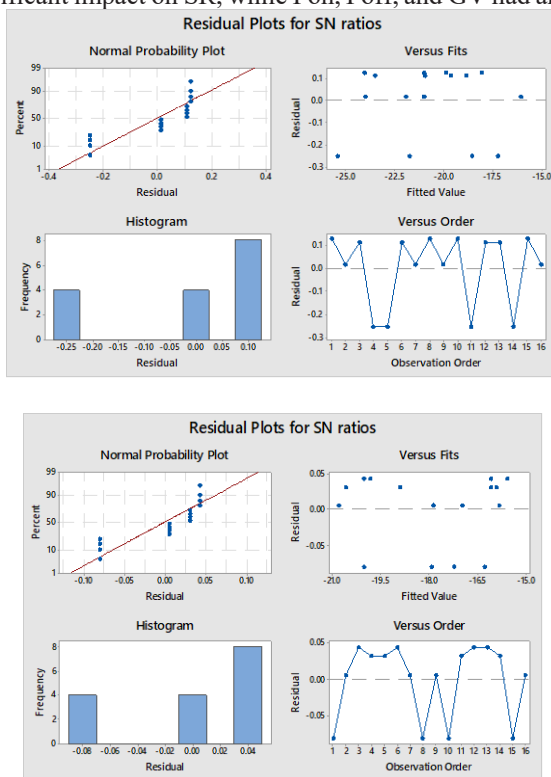


**Figure 7** Residual Plots of MRR & SR.

The normality of the experimental data was checked using normal probability plots. Figure 7 display the residual normal probability plots for MRR and SR of AHMMNC. The generated plots indicate that the residual values are clustered closer to the straight line,

indicating that the output values are in close proximity to the normal probability line. These plots were generated by plotting the residuals against the run orders to determine the independence of the experimental data for MRR and SR. The absence of any noticeable patterns in the two output variables validates that there is no correlation between them.

**Table 10** Results of authentication test.

S No.	Responses	Optimum condition	Predicted value	Experimental value	Error %
1	MRR	A <sub>4</sub> B <sub>4</sub> C <sub>1</sub> D <sub>1</sub>	0.1574	0.1601	1.68
2	SR	A <sub>1</sub> B <sub>1</sub> C <sub>4</sub> D <sub>4</sub>	5.3526	5.4523	1.91

### 3.4. Authentication Test

The confirmation experiments were carried out using the Taguchi technique to verify whether the predicted improvements based on the optimal control variables are observed. This is the final step in the process. According to the experimental results, the optimal combination of control variables for achieving maximum MRR is A<sub>1</sub>B<sub>1</sub>C<sub>4</sub>D<sub>4</sub>, while the optimal combination for maximum SR is A<sub>4</sub>B<sub>4</sub>C<sub>1</sub>D<sub>1</sub>. The authentication tests were carried out to validate the experimental and predicted values, and the results are presented in Table 10. Additionally, SEM micrographs of the machined surfaces of AHMMNC were obtained and presented in Figure 8 as part of the validation process. These results demonstrate the effectiveness of the selected combination of control variables in achieving the desired machining outcomes. It is observed that EDM process creates intricate mixture enclosed by small and large drops of the melts, different sizes of cracks and marks of void. In the EDM route, various particles were eroded and enclosed to the surface of the molten material is ejected indiscriminately due to that uneven EDMed surface structures were found. The *I<sub>p</sub>* is the most impacting variable and it enhances with high discharge energy creating deeper craters. This outcome in huge amount of molten material and floating metal is suspended in the machining zone resulting in deep and overlapping craters. Micro cracks formation on the surface is attributed to the occurrence of thermal stress and tensile stress. The uneven surface structure was seen on the figure.

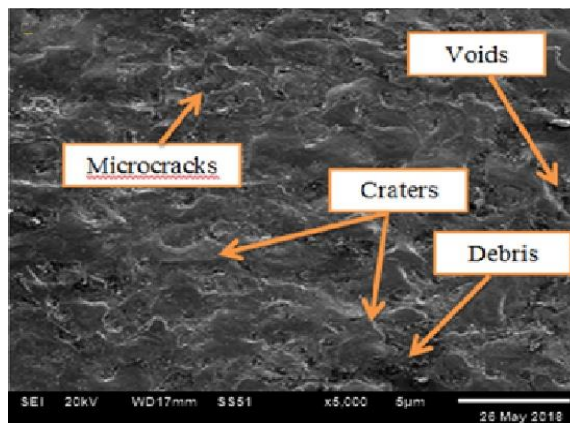


**Figure 8.** SEM image of EDMed surface of authentication test specimen.

### Conclusions

This study involved the production of a HMMNC composed of Al7010/B4C/BN using an UASC route. The optimal parameters for the EDM process of the developed AHMMNC were evaluated using the Taguchi method. The obtained results are presented below.

- The Taguchi method was successfully and efficiently incorporated to find the best control factors.
- The optimum input factors condition for maximum MRR is attained from Taguchi L16 orthogonal array is A1B1C4D4.
- The maximum SR condition was achieved by optimum input factors condition A4B4C1D1 from Taguchi L16 orthogonal array.
- The ANOVA test explains that the MRR is superior effected by DC (82.07%) followed by Pon (7.21%), Poff (6.60%) and GV (3.76%).
- The % of contribution of input variables are DC (91.71), GV (4.10), Pon (3.71) and Poff (0.40) were determined by ANOVA test in that most effecting factor on SR is DC.
- The SEM micrographs of optimum conditions of EDMed surface showed that voids, microcracks, craters were found.

## References

1. Reddy, A. P., Krishna, P. V., Rao, R. N., *Silicon*, **11**, 6 (2019)
2. Harichandran, R., Selvakumar, N., *Archives of Civil and Mechanical Engineering*, **16** (2016)
3. Dirisenapu, G., Reddy, S. P., Dumpala, L., *Materials Research Express*, **6**, 10 (2019)
4. Poovazhagan, L., Kalaichelvan, K., Sornakumar, T., *Materials and Manufacturing Processes*, **31**, 10 (2016)
5. Kumar, S. S., Uthayakumar, M., Kumaran, S. T., Varol, T., Canakci, A., *Defence Technology*, **15**, 3 (2019)
6. Singh, M., Dhuria, G., Garg, H. *International Journal for Science and Emerging Technologies with Latest Trends*, **20**, 1 (2015).
7. Palanisamy, D., Devaraju, A., Manikandan, N., Balasubramanian, K., and Arulkirubakaran, D., *Materials Today: Proceedings*, **5**, 9 (2018)
8. Gopalakannan, S., Senthilvelan, T., Ranganathan, S., *Procedia Engineering*, **38** (2012)
9. Daneshmand, S., Masoudi, B., *Silicon*, **10**, 3 (2018)
10. Nanimina, A. M., Abdul-Rani, A. M., Ahmad, F., Zainuddin, A., Lo, S. J., *Journal of Applied Sciences*, **11**, 11 (2011)
11. Kumar, P., & Parkash, R., **20**, 2 (2016)
12. Senthilkumar, V., Omprakash, B. U., *Journal of Manufacturing Processes*, **13**, 1 (2011)
13. Kathiresan, M., Sornakumar, T., *Journal of Minerals & Materials Characterization & Engineering*, **9**, 1 (2010)
14. Madhukar, P., Selvaraj, N., Gujjala, R., Rao, C. S. P. *Ultrasonics sonochemistry*, **58** (2019)
15. Dirisenapu, G, Dumpala, L, Seelam. P. R., *Materials Research Express*, **6**, 10 (2019)
16. Reddy, S. P., Rao, P. C., Kolli, M., *Journal of Testing and Evaluation*, **48**, 2 (2020)
17. Kannan, C., Vijayakumar, T., Karunakaran, C., *SAE Technical Paper*, (2018).
18. Singh, S., Bhardwaj, A., *Journal of Minerals and Materials Characterization and Engineering*, **10**, 2 (2011)
19. Kumar, S. S., Uthayakumar, M., Kumaran, S. T., Parameswaran, P., *Materials and Manufacturing Processes*, **29**, 11 (2014)
20. Sachit, T. S., Mohan, N., *Materials Research Express* **6**, 6 (2019)